ACS APPLIED ENERGY MATERIALS

Article

Spectrally Selective PANI/ITO Nanocomposite Electrodes for Energy Efficient Dual Band Electrochromic Windows

Pelin Yilmaz, Mirko Magni, Sandra Martinez, Rosa Maria Gonzalez Gil, Monica Della Pirriera, and Michele Manca

ACS Appl. Energy Mater., **Just Accepted Manuscript** • DOI: 10.1021/acsaem.0c00241 • Publication Date (Web): 26 Mar 2020

Spectrally Selective PANI/ITO Nanocomposite Electrodes for Energy Efficient Dual Band Dynamic Windows

Pelin Yilmaz,[a] Mirko Magni,*[b] Sandra Martinez,[c] Rosa Maria Gonzalez Gil,[c] Monica Della Pirriera,[c] Michele Manca*[a,c]

a. *IIT- CBN - Fondazione Istituto Italiano di Tecnologia - Center for Biomolecular Nanotechnologies, via Barsanti 14, 73010, Arnesano (Lecce), Italy – Corresp. Auth. michele.manca@iit.it*

b. *Dipartimento di Chimica, Università degli Studi di Milano, Via Golgi 19, Milano, Italy - Corresp. Auth. mirko.magni@unimi.it*

c. *LEITAT Technological Center, Carrer de la Innovació 2, 08225, Terrassa (Barcelona), Spain*

KEYWORDS: smart dynamic window, dual band electrochromic device, NIR transmittance, ITO plasmonic nanocrystals, polyaniline.

Electrochromic materials are able to dynamically and reversibly change their color due to oxidation or reduction reactions as a response to an external electrical stimulus. Glazing employing these materials can thus change their optical characteristics of transparency and absorption of solar radiation according to users' needs, by simultaneously reducing visible light and NIR transmission through the window. Spectral selectivity is now becoming a key issue in the development of smart dynamic glazing systems that are capable of maximizing both visual and thermal comfort while minimizing the energy consumption for heating, cooling and lighting.

An effective dual band electrochromic system is here presented, which consists of an engineered nanocomposite electrode that advantageously combines the broad band plasmonic features of nanocrystalline indium-tin-oxide with the high optical contrast of polyaniline. Their synergistical spectroelectrochemical features makes possible the implementation of a fully four-state tunable electrochromic device (here referred as “plasmochromic”), which permits to selectively regulate the optical transmittance in the visible and in the near-infrared range and exhibits an excellent spectral selectivity over a

narrow bias potential window: the ratio between visible light transmittance (T_{LUM}) and solar transmittance (T_{SOL}) can be tuned from 0.67 to 1.61 across a potential window of 1.2V.

1. INTRODUCTION

Chromogenic materials are able to change their optical properties as a response to an external stimulus, such as light irradiation (photochromic materials),[1,2] temperature variation (thermochromic materials)[3,4] or electric potential (electrochromic materials).[5,6] They have been long considered as a subset of the "solar energy materials", despite their potential enormous benefits in terms of energy savings and sustainability in pivotal sectors such as buildings and transportation.

Among them, electrochromic (EC) materials stand out as the most suitable candidates, as they offer to modulate optical transmittance over a broader spectral range by means of a user-defined control and enable the combination of two features that are often thought of as incompatible: energy efficiency (because of the curtailing of air conditioning) and indoor comfort (due to reduced glare and thermal discomfort).[7] Recently, mainly due to the unprecedent developments in the field of near-infrared (NIR) plasmonic EC materials, it has become widely clear that intelligent dynamic windows may provide up to 45% energy use reduction compared with conventional static solar control coatings.[8] Pioneering scientific works from Milliron's group[9-11] have in fact paved the way to the realization of a new class of EC systems capable of selectively shielding solar thermal loads without significantly affecting the visible light transmittance (T_{LUM}). They first reported the reversible electrochemical tunability of localized surface plasmon resonance (LSPR) features of a thin film of tin-doped indium oxide (ITO) nanocrystals (NCs) embedded into Li^+ salt containing liquid electrolyte (LE). Upon applying a negative bias, they recorded a remarkable blue-shift of the LSPR peak and a consequent reduction of

the overall transmittance in the NIR range.[12] This effect has been associated with a purely capacitive charging mechanism (excluding the intercalation effects) with the magnitude of the shift across the applied bias modulation being dependent on film thickness, NC size, surface trap density and doping level, since it is reasonably proportional to the concentration of Drude-type free carriers on the surface of transparent conductive oxide NCs. Cations from electrolyte neutralize the excess of charges on the NCs that are located at the electrode surface, within the pores and channels, or ideally around each particle within the film. The application of a small positive potential easily reverses the optical changes and even induces a red-shift of the LSPR with respect to its equilibrium position, causing a further enhancement of the optical transmittance in a relatively wide spectral window.

Referring to "traditional" color-switchable EC materials, it is also worth mentioning a wide class of organic compounds that have gained great research interest from both academia and industry, due to their ease of processability, rapid response times and high optical contrasts: it is the case of conjugated EC polymers,[13] which are generally constituted by a repetitive backbone unit alternating single and double (or even triple) bonds that impart the typical semiconductor behavior to the polymer.[14] In conjugated polymers electrochromisms occurs through changes in the molecular, and hence electronic, structure of the π-conjugated conducting skeleton upon electrochemical oxidation and reduction -also referred as electrochemical doping. Doping results into lower energy intraband transitions and polaronic/bipolaronic states of charge carriers, which ultimately determine reversible changes in their optical and electrical properties.[15] Among the abundant variety of EC conjugated polymers, derivatives of poly(thiophene) (PTh),[16] poly(pyrrole) (PPy),[17] and poly(aniline) (PANI)[18] are the most widely studied.

PANI, in particular, has been abundantly employed -not only in the field of electrochromisms- thanks to its many advantageous prerogatives such as ease of synthesis, accessible price and high stability compared to other conducting polymers.[19] PANI is a mixed oxidation state polymer composed of two distinct repeating units, reduced benzoid and oxidized quinoid ones.[20,21] The relative abundance of one of the two units determines the actual oxidation state of PANI and, hence, its electrical and optical properties. The redox state can spread from fully reduced leucoemeraldine (100% benzoid units), to half oxidized emeraldine (50% benzoid and 50% quinoid ones) and to fully oxidized pernigraniline (100% quinoid units), but all intermediate states can co-exist.[22,23] In contrast with other conducting polymers, which exhibit a p-doping induced switch between two-state of conductivity (insulating versus conducting), PANI exhibits a three-state conductivity (insulating-conducting-insulating), each state with its own inherent color, therefore offering a multi-colored EC behaviour.[24] Moreover, a peculiar property of PANI is that doping can occur not only by changing the oxidation state of the π-system (i.e. common p-doping, like with other traditional conducting polythiophene, polypyrrole, etc.) but also by changing pH of the aqueous medium which reflects on the protonation degree of the material (i.e. non redox doping).[25] This makes PANI a valuable platform to construct hybrid functional materials with properties going beyond the simple sum of the features of each component.

Multicolor EC systems based on composite/hybrid materials via the donor–acceptor approach have also been attracting great attention over the last decade.[26-28] Several research attempts have been dedicated to incorporate metal oxides such as WO_3,[29] TiO_2,[30] and NiO[31] into conjugated polymers to form organic/inorganic composite films with the motivation of enhancing the EC properties of the hybrid in terms of switching speed and stability thanks to interfacial interactions between the two components.

However, one of the most relevant benefits of hybrid EC nanocomposites relies on the possibility to combine two or more components displaying different (possibly complementary) spectroelectrochemical features and, ultimately, the possibility of independently and selectively controlling visible light and solar heat transmittance through the sign and the intensity of the applied bias voltage. These systems promise to enable the development of a new generation of intelligent dynamic glazing technologies capable of maximizing both the visual and thermal comfort and minimizing the energy loses for overheating and overcooling.[32] To this respect, several different combinations of EC materials have been explored in the recent years to design engineered dual band nanocomposite blocks: Llordes et al.,[9] for instance, introduced ITO nanocrystals into a niobium oxide (NbOx) matrix to obtain an amorphous composite with peculiar EC functionalities. Barile et al.[33] used instead a polythiophene matrix to disperse ITO NCs and modulate the optical properties of the nanocomposite film in VIS region by electrochemically doping the conjugated polymer and switching the film between three distinct modes of operation. Our research group recently also contributed to this subject by employing V-modified TiO_2 colloidal NCs as EC electrode selectively operating in the VIS range facing a WO_X nanocrystalline electrode capable of selectively modulate NIR transmittance.[34]

Despite the rapidly growing interest in these systems, several technical concerns still need to be addressed. In particular: i) spectral selectivity achieved so far is still insufficient as values of the change-over potentials cannot be sharply defined and the switching from an

optical state to another is in most of the cases overlapped; ii) visible light transmittance (T_{LUM}) cannot be selectively (and independently) regulated while maintaining high the NIR transmittance.

Starting from these considerations, we propose a viable approach to realize a batch of hybrid "plasmochromic" electrodes that can symbiotically combine the wide tunability in the NIR of ITO plasmonic NCs with the colorful fingerprints of PANI. Their inherent charge transfer phenomena at the PANI/ITO interface have been elucidated by cyclic voltammetry and electrochemical impedance spectroscopy. The most relevant outcomes have been finally adopted to design a set of dual-band EC devices offering an excellent VIS/NIR spectral selectivity within a relatively small electrochemical window.

2. EXPERIMENTAL DETAILS

Fabrication of ITO mesoporous films. 10 nm-sized colloidal ITO NCs were synthesized according to a previously reported surfactant-assisted sol-gel procedure:[36] 3 ml of ITO suspension (In_2O_3:SnO_2 90:10, 30 wt% in ethanol, Avantama™) were mixed with 5 ml of α-terpineol and 0.65 g of ethyl cellulose to prepare a suitably viscous slurry, which was subsequently deposited by doctor-blade on a 1 cm^2 area on an ITO-coated glass substrate (20 Ω/sq). The films were subjected to a thermal treatment in air at 430°C for 90 min (after two intermediate 30 min heating steps at 130°C and 250°C).

Electrodeposition of PANI. PANI films were obtained by electrochemical polymerization of 0.5 ml of aniline monomer (ReagentPlus®, 99% from Sigma Aldrich) in 50 ml of a 0.5 M H_2SO_4 aqueous solution. Electrodeposition was performed in a three-electrode cell through an Autolab PGSTAT 302N potentiostat by using ITO-coated glass (20 Ω/sq) as active electrode, a Pt mesh as counter electrode and AgCl/Ag (saturated in 1 M $LiClO_4$ in PC solution) electrode as reference. Different series of depositions were conducted, by

varying both the sweep rate and the number of cycles, to control thickness and homogeneity of the film.

Electrochemical characterization. Cyclic Voltammetry (CV) analyses were conducted at different scan rate potentials, with an electrolyte solution of 1 M $LiClO_4$ in propylencarbonate (PC). Pt foil/wire and AgCl/Ag (saturated in 1 M $LiClO_4$ in PC solution) were used respectively as counter electrode and reference electrode over the CV analysis. Aqueous saturated calomel electrode (SCE) was instead used as reference electrode over the EIS analysis. SCE was inserted into a glass jacket ending with a porous septum (i.e., double bridge) filled with the same working medium; in this way leakage of chloride and water into the working solution is significantly reduced. The electrolyte solution within the sealed electrochemical cell was purged with N_2 gas for 15 minutes before the tests. For sake of clarity, all the reported potentials are referred to a unique reference electrode (i.e., saturated AgCl/Ag) by adding 0.045 V to experimental potentials referred to SCE. Electrochemical surface area (ECSA) of bare and PANI-modified ITO electrodes was determined measuring double layer capacitance, C_{dl}, by performing cycles around the open-circuit potential, OCP, in a narrow potential window (+/– 50 mV around OCP) at different scan rate potentials.[37] The slope of the anodic and cathodic currents as a function of potential scan rate is equal to $C_{dl}=ECSA*C_s$, with C_s the specific capacitance of the material. In our case C_s is unknown, to the best of our knowledge, so only relative ECSA is accessible.

Electrochemical impedance spectroscopy, EIS, was carried out with an Autolab PGSTAT 302N potentiostat equipped with a frequency response analyzer. The bias potential was applied for 30 seconds before starting spectrum acquisition (equilibration time was estimated from potential-step chronoamperometry). EIS spectra were recorded using sinusoidal single sine signals with frequency ranging from 10^4 to 10^{-1} Hz, with 10 mV

amplitude. Data fitting was done with NOVA 1.10 software, choosing a proper equivalent circuit. Stability of the film was tested by recording CV after each spectrum acquisition. All electrochemical quantities reported in Figures (*i.e.* currents, resistances and capacitances) were normalized for the geometric area of the electrode, if otherwise stated.

Spectro-electrochemical characterization. Transmittance spectra of the films were measured in-situ in a Varian Cary 5000 spectrophotometer coupled with the PGSTAT 302N potentiostat. The electrodes were placed in a three-electrode electrochemical quartz cell positioned within the spectrophotometer, where Pt foil and Ag wire served as counter and pseudo-reference electrodes, respectively. Potentials are then referred to AgCl/Ag reference electrode considering redox potential of Ag pseudo-reference be around 0.40 V with respect to saturated aqueous AgCl/Ag. A solution of 1 M $LiClO_4$ in PC was used as the electrolyte. The measurements were performed in a wavelength range of 1600 to 350 nm, at which the baseline was set on the spectral response of the flat ITO coated glass substrate within the electrolyte. Switching kinetics of the films have also been investigated through transmittance measurements at both VIS and NIR wavelengths as a function of time upon charging and discharging at different square-wave switching potentials.

Fabrication of lab-scale EC devices. A set of lab-scale sandwich EC devices were fabricated using the PANI/ITO nanocomposite film as active working electrode and a mesoporous CeO_2 film (thickness ~350nm) as counter electrode. CeO_2 film was deposited by doctor blading on commercial ITO-coated glass slide by using a CeO_x-based sol-gel paste prepared according to the recipe provided in ref. 37. The electrodes were assembled in sandwich configuration with hot-melt 50µm-thick plastic paraffin film in between used as a mask. 1 M $LiClO_4$ solution in PC was used as electrolyte. It was introduced through

a small hole drilled on the counter electrode and the hole was then sealed by a thermosetting resin.

3. RESULTS AND DISCUSSIONS

PANI films were grown onto ITO-coated glass through potentiodynamic electro-oxidation of aniline in 0.5 M H_2SO_4 within a potential window comprised between -0.2 V and +1.3 V (vs AgCl/Ag). Continuous potential cycling was preferred to potentiostatic deposition as it has been proven to guarantee a better adhesion of the growing film, while choice of H_2SO_4 was dictated by the higher porosity achievable compared to smoother surfaces reported with other inorganic acids (i.e. HCl and $HClO_4$).[38-40] Current-potential plots of the first three scans recorded over an electro-deposition test conducted at a scan rate of 50 mV/s are displayed in **Figure 1a**. Upon applying a positive potential corresponding to the required activation energy (around 1.2 V vs AgCl/Ag), the aniline monomer is oxidized to the corresponding radical cation and the polymerization reaction is triggered.[39] Three distinctive redox processes come to be observed hereafter, which testify the potential-driven oxidation of the growing PANI from the reduced leucoemeraldine state to the partly oxidized emeraldine state (at 0.1V vs AgCl/Ag) followed by oxidation to pernigraniline (at 0.7 V vs AgCl/Ag). The intermediate peak is ascribed to partial oxidation of aniline species during the electropolymerization. The continuous increase in the intensity of the reduction peak on the subsequent cycles and the concomitant broadening and upshift of the oxidation peak mark the film's growth.[40]

The chemical fingerprints of the as-prepared films are highlighted in the FTIR spectra reported in **Figure S1** (see ESI section); the characteristic peaks observed at 1574 and 1487 cm^{-1} confirm the presence of quinoid ring and benzenoid ring vibrations, respectively. The absorption peaks at 1296 and 1244 cm^{-1} are instead attributed to the C–

N stretching vibration of the aromatic amine and the absorption peak at 1134 cm^{-1} to the in-plane aromatic C–H bending. The latter is described as the "electronic-like band" characteristic of conductive PANI and exhibits the extent of electron delocalization. The band at 799 cm^{-1} has been ascribed to the out of plane bending vibration of C–H in the aromatic ring.[29]

Several batches of PANI were prepared by varying either scan rate and number of cycles to obtain different combinations of thicknesses and molecular weights. A representative SEM image of a film obtained after 3 cycles at 50 mV/s is shown in **Figure 1b**: average thickness is around 150 nm. Its electrochemical fingerprints have been documented through a CV analysis conducted at 100 mV/s in PC with 1M LiClO4 as supporting electrolyte (see **Figure 1c**): two well-defined peak couples are revealed, addressing the corresponding chemically reversible redox transitions among the previously referred PANI oxidation states, starting with the oxidation of leucoemeraldine (100% benzoid units) to emeraldine (50% benzoid and 50% quinoid units) at +0.1 V and then to pernigraniline (100% quinoid units) at +1.0 V vs AgCl/Ag. Both two transitions are fully reversible (films turned back to leucoemeraldine upon the cathodic scan) and revealed a pseudo-capacitive behavior typical of solid-state redox processes (a linear correlation between peak currents and scan rate potential has been revealed as documented in **Figure S2**). In the emeraldine state PANI exhibits instead a predominantly capacitive behavior (**Figure S3**, see ESI), which can be attributed to positive charge accumulation in the polymer matrix.

The corresponding optical features were inspected by positioning a three-electrode quartz cell in the spectrophotometer case and recording spectra while keeping the PANI-coated electrode at different potentials. A few representative absorption spectra are plotted in **Figure 1d**. At its fully reduced state (leucoemeraldine, potentials lower than ca. -0.2 V

vs AgCl/Ag), PANI shows an intense absorption peak at ~340 nm which is attributed to π-π* transition at its benzoid units. Leucoemeraldine displays a typical green color and low absorption intensity in both VIS and NIR. The film can be even bleached to a highly transparent state at further negative potentials (around –0.5 V vs AgCl/Ag,). Upon oxidation to the emeraldine state (at +0.1 V vs AgCl/Ag) the film evolves into blueish tone and manifests a broad NIR absorption band that is associated with the formation of localized bipolaron states.[25] At higher positive potentials (> +1.0 V vs AgCl/Ag), it finally takes a violet color, corresponding to the fully oxidized pernigraniline state. A high absorption peak is detected around ~620 nm that can be reasonably associated to electronic transitions involving quinoid units instead of benzoid,[41] which is accompanied to the vanishing of NIR absorption band.[25,42] The corresponding color changes observed over the above-mentioned transitions are highlighted in the inset of **Figure 1d**.

A systematic EIS analysis has been carried out to highlight the variation of some relevant electrochemical parameters behind the redox color tuning. Details are given in the ESI section (see also **Figure S4**), including a description of the equivalent circuit used in the fitting procedure. Results of the numerical fitting of EIS spectra recorded at different applied potentials for a ~150nm PANI on flat ITO are given **Figure 2a** and **2b**. While the series resistance, R_S, mainly accounting for the electrolyte resistance remains constant throughout the potential window, the polarization resistance, R_P, associated to the mobility of charge carrier in the polymer chains, drastically decreases upon the leucoemeraldine-emeraldine transition then reaching a constant value between 0.2 and 0.4 V (vs AgCl/Ag) and finally increasing at more positive potentials.[43] Both shape and magnitude of R_P variation well fit the expected behavior for a three-state conductivity material that is electrochemically doped by progressively applying a more positive potential, according to the following reaction pathway:

$$leucoemeraldine \xrightarrow[-e^{-}(\sim +0.1V)]{} emeraldine \xrightarrow[-e^{-}(\sim +1.0V)]{} pernigraniline$$

A lower mobility of charge carriers (i.e, higher R_P) is expected in both leucoemeraldine and pernigraniline less conductive states than in conductive emeraldine one. According to this potential-driven transition, the so called redox pseudo-capacitance, C_{redox} (calculated from CPE_2 element, see ESI), typical of polymer in their conducting state, sharply increases up to a maximum stationary value around 1 mF cm^{-2} (**Figure 2a**). This net increase of C_{redox} perfectly matches with the occurring of the first redox process, centered around 0 V vs AgCl/Ag, associated to the switch from the low conductive (leucoemeraldine) to more conductive (emeraldine) state of PANI. In the conductive state PANI behaves as a capacitor upon application of medium/low frequency potential perturbation, the typical time scale of voltammetry experiments and, as a limiting situation, of potentiostatic polarization. Due to the transfer of electrons to the ITO substrate, counterbalanced by anion/cation ingress/egress to/from polymer matrix, accumulation of positive charges occurs on PANI as no electron transfer can occur at the PANI/electrolyte interface, due to the absence of any redox probe into the electrolyte. Fitted values of the double layer capacitance C_{DL} (derived from CPE_1 element, see ESI) lay around few µF cm^{-2}, a typical value of electric double layer of electrolytes and space charge of semiconductors. Both the values and the trend with potential are in good agreement with literature results.[39] Mott-Schottky representation of the C_{DL} is given in **Figure 2b**, where the C_{DL}^{-2} vs V plot exhibits a clear symmetric peak, centered at 0.30 V (vs AgCl/Ag), which can be likely attributed to the formation of an inversion layer in the space charge region of the semiconducting polymer. Keeping in mind the quite strong approximations associated to this kind of analysis, the flat band potential (of the valence band) of the organic film can be roughly estimated around 0.60 V (vs AgCl/Ag), in good agreement with previously reported measurements.[44] The Mott-Schottky analysis

performed on the pristine flat ITO within the same experimental conditions points to a n-type semiconductor behavior and a flat band potential of around –1.0 V (vs AgCl/Ag, **Figure S5**, see ESI). Therefore, the Fermi level alignment at the interface between the p-type (i.e., PANI) and the n-type (i.e., ITO) semiconductor can bring to the formation of a p-n heterojunction that favors movement of charge carriers.

Thereafter a second set of samples was prepared by using nanocrystalline ITO mesoporous films (ITO NCs) as growing platform for the fabrication of nanocomposite films. Mesoporous ITO films were prepared according to the procedure described in a previous work.[35] They are featured by a specific surface area in the order of 180 m^2/g. **Figure 3a** shows the CVs recorded over the electropolymerization of aniline carried out at 50 mV/s on mesoporous ITO film over the first three scans. Characteristic anodic peaks of the growing PANI (at about 0.2 V and 0.7 V vs AgCl/Ag) can be identified although not sharply defined as in the case of PANI deposited on flat ITO. The "elongated" shape of the grown pattern, if compared with that on flat ITO, could be reasonably attributed to the higher intrinsic transport resistance across the ca. 1 μm thick NCs film with respect to the commercial flat ITO coating, as also confirmed by EIS analysis (**Figure S6**, see ESI). As a result, the potential drop could explain the higher distance between forward and backward peak potential for the two redox processes.

Upon electropolymerization of PANI onto ITO-NCs, the FTIR analysis conducted on the nanocomposite film confirms the interfacial interactions between the ITO NCs and the PANI chains as almost all the peaks of PANI have shifted to lower wavenumbers (**Figure S1**, see ESI). These shifts, such as from 1296 to 1292 cm^{-1} for C-N stretching mode of quinoid rings or from 799 to 795cm^{-1} for C-H bending in the aromatic ring, could be ascribed to constraints and deformations upon formation of a composite structure, an indicative of new covalent bindings between PANI and ITO. Similar results have been

also reported for analogue composites, where PANI was bonded to other inorganic matrices such as TiO_2, NiO and WO_3.[9, 45] **Figure 3b** and **3c** show the SEM images of an ITO NCs electrode respectively before and after the electro-deposition of PANI. The polymer homogeneously covers the mesoporous ITO surface while the porous structure is still partially preserved, as confirmed by values of the electrochemical surface area (ECSA) calculated from double layer capacitance (**Figure S7**, see ESI).[36] CVs of bare nanocrystalline ITO, PANI on flat ITO-glass and PANI/ITO nanocomposite (measured at the same conditions) are reported for comparison in **Figure 3d**. The typical redox PANI's fingerprints are clearly identifiable when it is deposited on flat-ITO. Porous nanocomposite rather exhibits a remarkable capacitive behavior, while the PANI peaks can be still traced. The higher current with respect to PANI on flat ITO is due to the aforementioned increase of active surface area of the composite. As a result, the nanocomposite electrode conveniently embodies the complementary electrochemical features arising from each of two constitutive building blocks, namely high surface capacitance from the inorganic scaffold (at more negative potential) and intense redox activity from the polymeric filler (at more positive potential).

EIS analysis on the PANI/ITO NC films revealed their predominant capacitive behavior, as attested by the Bode diagrams given in **Figure 4a**. Hybrid PANI/ITO NC exhibits indeed a neat semicircle in a complex capacitance plot (**Figure S8**, see ESI), whose diameter is function of the applied potential. Differently from what previously observed on flat PANI, the peak in the high/medium frequency range in the Bode plot (**Figure 4a**), associated to charge transfer resistance, is here not clearly detectable. This points to a much faster electron transfer at PANI/ITO interface as effect of the larger contact area and, possibly, of the good electrical connection at the organic/inorganic interface resulting from the strong chemical bonds between ITO NCs and PANI. Hence in this

case, EIS spectra can be simply fitted through a resistance connected in series with a CPE. The limiting capacitance (**Figure 4b**) qualitatively resembles the trend observed with PANI on flat ITO, although it shows consistently larger values: maximum capacitance is obtained with PANI in the emeraldine state (ca. 5 mF cm^{-2}) while drops occur at the more extreme potentials in both directions, situation corresponding to switching to leucoemeraldine and pernigraniline forms (**Figure S9,** see ESI). The higher redox capacitance of the nanocomposite can be mostly ascribed to its higher active surface area as evident from the comparison of normalized values (**Figure S10**, see ESI).

The most meaningful spectro-electrochemical features of the PANI/ITO NC electrode are reported in **Figure 5**. As previously documented,[35] bare nanocrystalline ITO displays a broad tuning of the optical density in the NIR range, which is associated to a reversible modulation of LSPR scattering. Transmission spectra of the 1.2μm-thick nanoporous electrode used as template for the electrodeposition of PANI are given in **Figure 5a**. It exhibits a wide tunability in the range from 900nm to 1600nm as response to the application of a moderate cathodic potential (till -0.6 V vs AgCl/Ag) and ultimately reaches a maximum ΔT of ~80% at 1600nm. Due to the formation of an increasingly denser electron accumulation layer on the surface of ITO NCs, the film undergoes a blue-shift -and a concomitant intensification- of the LSPR scattering, which can be easily up-reversed by inverting the polarity of the applied bias. Upon the electrodeposition of PANI, a hybrid dual-band EC system comes to be formed, which is thereafter referred as a "plasmochromic", as it embodies the spectral responses of two materials in a complementary fashion (i.e., plasmonic resonance of ITO NCs and electrochromism of PANI). Its transmittance spectra are displayed in **Figure 5b**. According to the electrochemical activity of the two components, at moderate positive potentials PANI dominates the EC response of the nanocomposite, whereas LSPR scattering at the

ITO/electrolyte interface prevails at higher negative voltages. The "plasmochromic" film thus displays four distinct optical regimes determined by as many bias potential intervals, namely:

- the as deposited PANI film is in slightly oxidized emeraldine state with a typical light blue color. By slightly oxidizing it (e.g., 0.5 V vs AgCl/Ag), the spectrum presents a peculiar NIR-selective cut-off due to bipolaron absorption accompanied with a relatively high transparency in the green/red spectral range. This optical state is referred as "NIR BLOCKING";

- at moderate negative potentials (i.e., –0.4 V vs AgCl/Ag) the film recovers a considerably high transparency over the whole measured spectral range (in this state the electrode can be thus referred as "FULLY TRANSPARENT") as PANI is completely reduced to leucoemeraldine, but the potential is not high enough to induce a significant LSPR modulation on the surface of ITO NCs.

- at higher negative voltages (up to –1.0V vs AgCl/Ag), electrons accumulation on ITO surface becomes more consistent and a wide attenuation of the optical transmittance in the NIR region (from 800nm to 1600nm) comes to be observed, while VIS transparency remains unchanged as PANI maintains completely bleached in its leucoemeraldine state. This state is referred as "BRIGHT"

- carrying polarization on the other side, at moderate positive potentials, PANI gets colored and progressively changes from blue (typical of the emeraldine state) to violet (typical of pernigraniline). VIS transparency thus drops off while a gradual recovery in the NIR range comes to be observed at potentials higher then +1.2V, which is associated with the lack of IR-active bipolaron states. This state is referred as "VIS BLOCKING".

In **Figure 5c** the spectral distribution of the solar irradiance (under the AM1.5 filter) is reported together with the three meaningful spectra corresponding to the use of the

"plasmochromic" filters at three specific operative conditions referred above (namely FULLY TRANSPARENT, NIR BLOCKING, VIS BLOCKING). The corresponding values of T_{LUM}, T_{SOL} and T_{NIR} are given in **Table 1**: as observable the T_{LUM}/T_{SOL} ratio sweeps from ~0.67 to ~1.61, passing through the fully transparent state (T_{SOL}/T_{LUM} ~1), which is associated with both high T_{LUM} and T_{NIR}.

Switching kinetics have also been studied by monitoring the transmittance variation upon charging and discharging the film through the application of a square wave switching potential at three different wavelengths. Meaningful plots are reported in **Figure 5d**: at 500 nm between OCP and +0.8 V vs AgCl/Ag; at 600 nm between –1.0 V and +1.2 V vs AgCl/Ag; at 1000 nm between +1.2 V and +0.6 V vs AgCl/Ag. The switching time, defined as the time required for 90% change in the transmission between the states, has been calculated at three different optical states. The coloring time, t_c, was found to range from ~4 s (at 600 nm) to ~19 s (at 500 nm) mainly depending on the intensity of the switching potential, whereas, the bleaching time, t_b, ranged from ~6 s at 500 nm to ~28 s at 1000 nm (see **Table 1**). The fast switching kinetics of the NC electrode can be attributed to the efficient charge transfer occurring at the interface between the PANI chains and the ITO nanocrystalline film, as referred above through EIS analysis. The fast kinetics is responsively due to the structural networking upon after the formation of extra covalent bonds among the two components.[33]

The PANI/ITO "plasmochromic" film was finally adopted as optically active electrode in a set of lab-scale sandwich test cells having the following architecture: glass_ITO/PANI-NCs/Electrolyte/CeO_2/ITO_glass, namely sandwich test cells embodying a mesoporous layer of CeO_2 (thickness ~350 nm) as optically passive counter electrode. **Figure 6a** displays the transmittance spectra of a representative test device within a wide interval of applied potentials (from –3.2 to +1.4V). According to the spectroelectrochemical

investigation, just discussed, two-states of NIR selectivity was revealed during both charging and discharging, each of which was due to EC features of one of the individual components. At negative potentials, the blue-shift of the LSPR peak is induced at ITO NCs offering a ΔT_{MAX} of 40% at 1600 nm ΔV= –2.4/-3.2 V). The NIR selectivity at the positive potentials, on the other hand, is due to the pernigraniline formation within the PANI layer resulting into bipolaron disappearance (ΔT_{MAX} = 60% at 1600 nm ΔV=+0.7/+1.4 V). For the visible range, the redox activity of PANI governs the optical modulation upon transformation from almost transparent leucomeraldine to violet color pernigraniline layer (ΔT_{MAX} = 60% at 600 nm, ΔV= –3.2/+1.4 V).

A key parameter for the evaluation of the performance of an EC device is the coloration efficiency (CE), which is defined as the change in optical density (ΔOD) per injected charge (ΔQ) at a fixed wavelength. **Figure 6b** shows the (ΔOD) versus (ΔQ) for the device upon switching between optical modes, where the slope of the line in the low charge region gives the CE value. At λ=1600 nm, the CE yielded 293 cm^2/C upon switching between –3.2 and –2.4V, whereas it was decreased to 60 cm^2/C at positive voltage switching of +1.4/+0.7 V. The value was 227 cm^2/C when calculated at λ=600 nm (–3.2/+1.4 V).

4. CONCLUSIONS

We have herein demonstrated a reliable approach to fabricate a dual-band EC system with high optical contrast and excellent spectral selectivity through the fabrication of a ITO/PANI nanocomposite electrode combining the redox EC response of polyaniline with the widely tuneable NIR plasmonic features of ITO nanocrystalline films. The near complementary electrochemical-driven response of the two components allows giving rise to four optical modes, which turns into a widely tuneable range of T_{LUM}/T_{SOL} values

(namely from 0.67 to 1.61) along with an as high ΔT as 80% in the NIR over a quite narrow potential window (about 1.2V). These remarkable optical features must be correlated with the high active surface area of the nanocomposite electrode as well as to the extremely low charge transfer resistance at the interface between ITO surface and PANI chains. An accurate analysis of the charge transfer and accumulation mechanisms regulating the spectro-electrochemical response of this system as well as an appropriate work of engineering and optimization may convert the here presented approach into an industrially viable solution for the development of a 2nd generation EC windows – which can be referred as "plasmochromic"- that are expected to fully address the issues of energy saving, visual and thermal comfort.

5. ASSOCIATED CONTENT

Electronic Supporting Information: FTIR analysis and additional detailed electrochemical analysis of the ITO nanocrystalline film, PANI film and ITO/PANI nanocomposite film. The Supporting Information is available free of charge on the ACS Publications website at DOI:

6. ACKNOWLEDGEMENTS

This work was partially supported by the Italian Ministry for Education, University and Research (MIUR) through the project SE4I (PON ARS01_01137 - Prot. n. 2060 02/08/2018) and by the Agency for Business Competitiveness of the Government of Catalonia (ACCIO') through the project SUNDANCING (TECNIOSPRING+ program / MSC grant agreement 712949). M. Magni gratefully acknowledges Prof. P. R. Mussini (Dep. of Chemistry, Università degli Studi di Milano) for getting access to the lab

facilities, and Fondazione Cariplo and Region Lombardia for funding his postdoc grant (2016-0923 RST).

7. REFERENCES

(1) Zhang, J.; Zou, Q.; Tian, H. Photochromic materials: more than meets the eye. *Adv. Mat.,* **2013**, 25, 378-399

(2) Pardo, R.; Zayat, M.; Levy, D. Photochromic organic-inorganic hybrid materials. *Chem. Soc. Rev*, **2011**, 40, 672-678

(3) Granqvist, C. G. Transparent conductors as solar energy materials: a panoramic review. *Sol. En. Mat. Sol. Cells*, **2007**, 91, 1529-1598

(4) Kamalisarvestani, M.; Saidur, R.; Mekhilef, S.; Javadi, F. S. erformance, materials and coating technologies of thermochromic thin films on smart windows. *Renew. Sustain. Energy Rev,* **2013**, 26, 353-364

(5) Monk, P. M. S.; Rosseinksy, D. R.; Mortimer, R. J. Electrochromic Materials and Devices Based on Viologens. *Electrochromic Materials and Devices*, Cambridge University Press, **2007**

(6) Niklasson, G. A.; Granqvist, C. G. Electrochromics for smart windows: Thin films of tungsten oxide and nickel oxide, and devices based on these. *J. Mater. Chem.*, **2007**, 17, 127–156

(7) Pacheco-Torgal, F.; Jalali, S. Nanotechnology: Advantages and drawbacks in the field of construction and building materials. *Constr. & Build. Mater*., **2011**, 25, (2), 582-590

(8) De Forest, N.; Shehabi, A.; O'Donnell, J.; Garcia, G.; Greenblatt, J.; Lee, Eleanor, S. L.; Selkowitz, S.; Milliron, D.J. United States energy and CO_2 savings potential from deployment of near-infrared electrochromic glazings. *Buildings and Environment*, **2015**, 89, 107-117

(9) Llordés, A.; Garcia, G.; Gazquez, G.; Milliron, D. J. Tunable near-infrared and visible-light transmittance in nanocrystal-in-glass composites. *Nature*, **2013**, 500, 323-326

(10) Runnerstrom, E. L.; Llordés, A.; Lounis, S. D.; Milliron, D. J. Nanostructured electrochromic smart windows: Traditional materials and NIR-selective plasmonic nanocrystals. *Chem. Commun*., **2014**, 50, 10555–10572

(11) De Trizio, L.; Buonsanti, R.; Schimpf, A. M.; Lordes, A.; Gamelin, D. R.; Simonutti, R.; Milliron, D. J. Nb-doped colloidal TiO2 nanocrystals with tunable infrared absorption. *Chem. Mat.*, **2013**, 25, 3383-3390

(12) Garcia G.; Buonsanti R.; Llordes, A.; Runnerstrom, E. L.; Bergerud, A.; Milliron, D. J. Near-Infrared Spectrally Selective Plasmonic Electrochromic Thin Films. *Adv. Opt. Mater.*, **2013**, 1, 215–220

(13) Long, Y. Z.; Lia, M. M.; Changzi, G.; Wan, M.; Duvaild, J. L.; Liue, Z.; Fan, Z. Recent advances in synthesis, physical properties and applications of conducting polymer nanotubes and nanofibers. *Prog. Polym. Sci.*, **2011**, 36, 1415-1442

(14) Le, T. H.; Kim, Y.; Yoon, H. Electrical and electrochemical properties of conducting polymers. *Polymers*, **2017**, 9, 150

(15) Argun, A. A.; Aubert, P. H.; Thompson B. C.; Schwendeman, I.; Gaupp, C. L.; Hwang, J.; Nicholas, J. P.; Tanner, D. B.; MacDiarmid, A. G.; Reynolds, J. R. Multicolored electrochromisin in polymers: Structures and devices. *Chem. Mater.*, **2004**, 16, 4401-4412

(16) Groenendaal, B. L.; Jonas, F.; Freitag, D.; Pielartzik, H.; Reynolds, J. R. PEDOT: Its Derivatives : Past , Present and Future. *Advanced Materials*, **2000**, 12, 481-494

(17) Schottland, P.; Zong, K.; Gaupp, C. L.; Thompson, B. C.; Thomas, C. A.; Giurgiu, I.; Hickman, R.; Abboud, K. A.; Reynolds, J. R. Poly(3,4-alkylenedioxypyrrole)s: Highly stable electronically conducting and electrochromic polymers. *Macromol.,* **2000**, 33, 7051-7061

(18) Gospodinova, N.; Terlemezyan, L. Conducting polymers prepared by oxidative polymerization: polyaniline. *Prog. Polym. Sci.*, **1998**, 23, 1443–1484

(19) Bhadra, S.; Khastgir, D.; Singha, N. K.; Lee, J. H. Progress in preparation, processing and applications of polyaniline. *Prog. Polym. Sci.*, **2009**, 34, 783–810

(20) Sabri, F. N.; Monajemi, H.; Zain, S. M.; Wai, P. S.; Rungrotmongkol, T.; Lee, V. S. Molecular conformation and UV–visible absorption spectrum of emeraldine salt polyaniline as a hydrazine sensor. *Integr. Ferroelectr.* **2016**, 175, 202-210

(21) Shimano, J. Y.; MacDiarmid, A. G. Polyaniline, a dynamic block copolymer: Key to attaining its intrinsic conductivity. *Synth. Met.*, **2001**, 123, 251.262

(22) Saini, P.; Arora, M. Formation mechanism, electronic properties & microwave shielding by nano-structured polyanilines prepared by template free route using surfactant dopants. *J. Mater. Chem. A*, **2013**, 1, 8926–8934

(23) Ciric-Marjonovic, G. Recent advances in polyaniline research: Polymerization mechanisms, structural aspects, properties and applications. *Synth. Met.*, **2013**, 177, 1-47

(24) Huang, W. S.; MacDiarmid, A. G. Optical properties of polyaniline. *Polymer*, **1993**, 34, 1833-1845

(25) R. J. Cushman, P. M. Mcmanus, S. C. Yang, Protonation and electrochemical doping of polyaniline: Correlation between the changes in electrical conductivity and optical spectrum. *Makromol. Chem. Rapid Commun.,* **1987**, 8, 69-75

(26) R.D. Rauh, F. Wang, J. R. Reynolds, D. L. Meeker, High coloration efficiency electrochromics and their application to multi-color devices. *Electrochim. Acta*, **2001**, 46, 2023–2029

(27) De Longchamp, D. M.; Hammond, P. T. Multiple-color electrochromism from layer-by-layer-assembled polyaniline/Prussian Blue nanocomposite thin films. *Chem. Mater.,* **2004**, 16, 4799-4805

(28) Ma, D.; Shi, G.; Wang, H.; Zhang, Q.; Li, Y. Controllable growth of high-quality metal oxide/conducting polymer hierarchical nanoarrays with outstanding electrochromic properties and solar-heat shielding ability. *J. Mater. Chem. A*, **2014**, 2, 13541-13549

(29) Wei, H.; Yan, X.; Wu, S.; Luo, Z.; Wei, S.; Guo, Z. Electropolymerized polyaniline stabilized tungsten oxide nanocomposite films: Electrochromic behavior and electrochemical energy storage. *J. Phys. Chem. C*, **2012**, 116, 25052–25064

(30) Lv, H.; Wang, Y.; Pan, L.; Zhang, L.; Zhang, H.; Shang, L.; Qu, H.; Li, N.; Zhao, J. Patterned polyaniline encapsulated in titania nanotubes for electrochromism. *Phys. Chem. Chem. Phys*., **2018**, 20, 5818–5826

(31) Sonavane, A. C.; Inamdar, A. I.; Deshmukh, H. P.; Patil, P. S. Multicoloured electrochromic thin films of NiO/PANI. *J. Phys. D. Appl. Phys*., **2010**, 43, 315102

(32) Wang, Y.; Runnerstrom, E. L.; Milliron, D. J. Switchable Materials for Smart Windows. *Annu. Rev. Chem. Biomol. Eng*., **2016**, 7, 283–304

(33) Barile, C. J.; Slotcavage, D. J.; McGehee, M. D. Polymer − Nanoparticle Electrochromic Materials that Selectively Modulate Visible and Near-Infrared Light. *Chem. Mater.*, **2016**, 28, 1439−1445

(34) Barawi, M.; Veramonti, G.; Epifani, M.; Giannuzzi, R.; Sibiliano, T.; Giannini, C.; Rougier, A.; Manca, M. A dual band electrochromic device switchable across four distinct optical modes. *J. Mater. Chem. A*, **2018**, 6, 10201–10205

(35) Pattathil, P.; Giannuzzi, R.; Manca, M. Self-powered NIR-selective dynamic windows based on broad tuning of the localized surface plasmon resonance in mesoporous ITO electrodes. **2016**, *Nano Energy*, 30, 242–251

(36) Trasatti, S.; Petrii, O. A. Real Surface Area Measurements in Electrochemistry. *Pure Appl. Chem*., **1991**, 63, 711–734

(37) Lundberg, M.; Skarman, B.; Cesar, F.; Reine Wallenberg, L. Mesoporous thin films of high-surface-area crystalline cerium dioxide. *Microporous Mesoporous Mater.,* **2012**, 54, 97–103

(38) Syed, A. A.; Dinesan, M. K. A. Review: Polyaniline - A Novel Polymeric Material. *Talanta*, **1991**, 38, 815-837

(39) Molapo, K. M.; Ndangili, P. M.; Ajayi, R. F.; Mbambisa, G.; Mailu, S. M.; Njomo, N.; Masikini, M.; Baker, P.; Iwuoha, E. I. Electronics of Conjugated Polymers (I): Polyaniline. *Int. J. Electrochem. Sci.,* **2012**, 7, 11859–11875

(40) Ninh, D. H.; Thao, T. T.; Ling, P. D.; Dinh, N. N. Characterization of Electrochromic Properties of Polyaniline Thin Films Electropolymerized in H_2SO_4 Solution. *J. Org. Polym. Mater.,* **2016**, 6, 30–37

(41) Rohom, A. B.; Londhe, P. U.; Chaure, N. B. Enhancement of Optical Absorption by Incorporation of Plasmonic Nanoparticles in PANI Films. *Nanosci. Nanotechnol.*, **2016**, 6, 83–87

(42) Padmapriya, S.; Harinipriya, S.; Jaidev, K.; Sudha, V.; Kumar, D.; Pal, S. Storage and evolution of hydrogen in acidic medium by polyaniline. *Int. J. En. Res.*, **2018**, 42, 1196-1209

(43) Zhang, J.; Tu, J. Multicolor electrochromic polyaniline–WO_3 hybrid thin films: One-pot molecular assembling synthesis. *J. Mater. Chem.*, **2011**, 21, 17316

(44) Das Neves, S.; Da Fonseca, C. N. P.; De Paoli, M. Photoelectrochemical characterization of electrodeposited polyaniline. *Synth. Met.*, **1997**, 89, 167–169

(45) Cai, G. F.; Tu, J. P.; Zhou, D.; Zhang, J. H.; Wang, X. L.; Gu, C. D. Dual electrochromic film based on WO_3/polyaniline core/shell nanowire array. *Sol. En. Mater. & Solar Cells*, **2014,** 122, 51–58

8. FIGURES

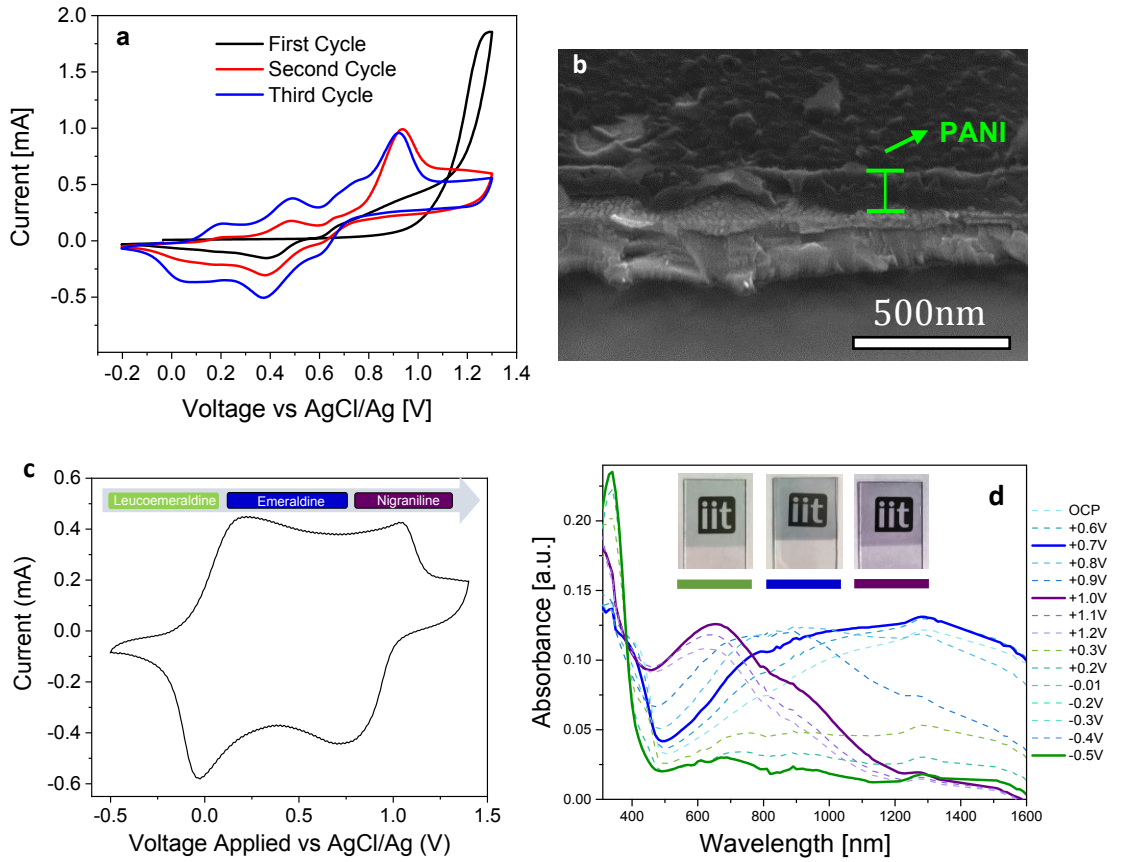

Figure 1. a) CV patterns recorded over the electro-polymerization at 50 mV/s in 50 ml of 0.5 M H_2SO_4 with 0.5 ml aniline on flat ITO coated glass substrate for 3 cycles; b) SEM picture of PANI film; c) CV pattern of PANI film on flat ITO coated glass substrate recorded at 100 mV/s in 1 M $LiClO_4$ in PC; d) absorption spectra of the same film at few representative applied voltages referred to AgCl/Ag. In the inset (top) the photographs of the PANI thin films at corresponding voltages are shown for demonstration of color change upon the potential-driven transition in between PANI oxidation states.

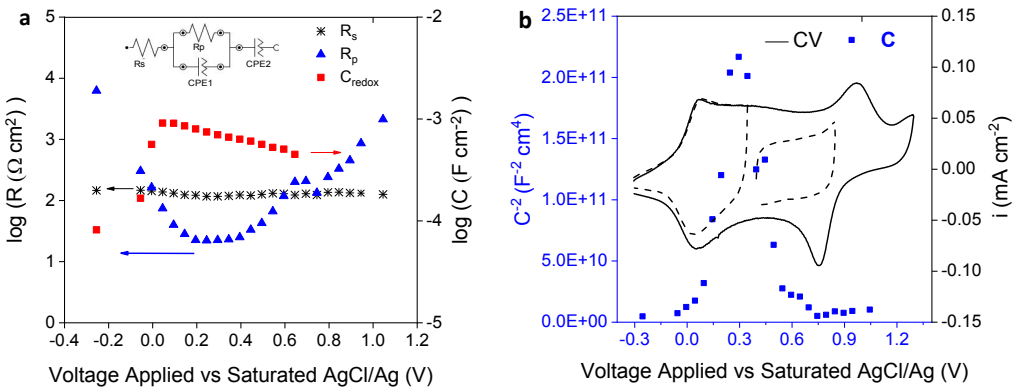

Figure 2. a) Variation of equivalent circuit components (inset) as a function of applied potential. b) Mott-Schottky representation of the capacitance C associated to CPE1 element. For sake of comparison CVs at 0.035 V s^{-1} are also reported. Normalization was done on the geometric area. Electrolyte: PC + $LiClO_4$ 1 M

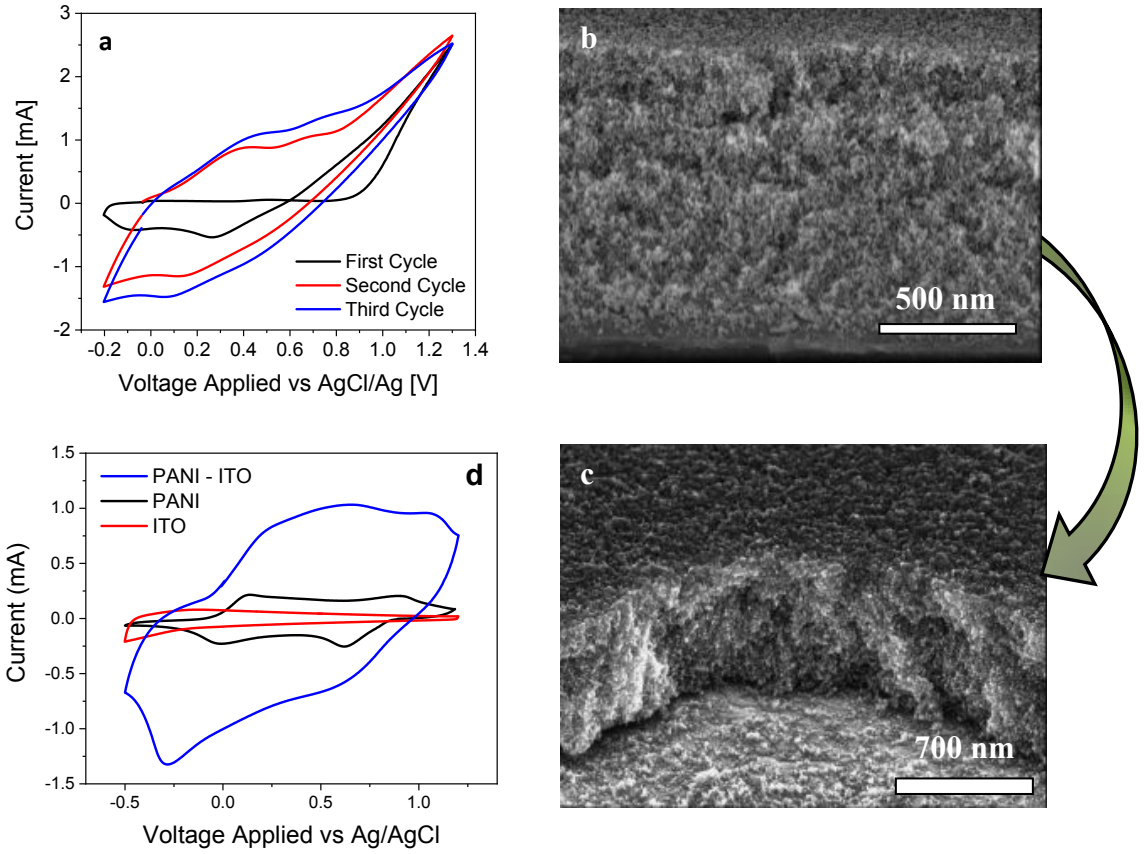

Figure 3. a) CV plots recorded over the electropolymerization at 50 mV/s in H_2SO_4 0.5 M on a mesoporous ITO electrode. SEM image of the ITO mesoporous electrode b) before and c) after the deposition of PANI. d) CV patterns recorded at 50 mV/s in 1M $LiClO_4$ in PC of PANI/ITO NC (blue line), ITO NCs (red line) and PANI on flat ITO (black line)

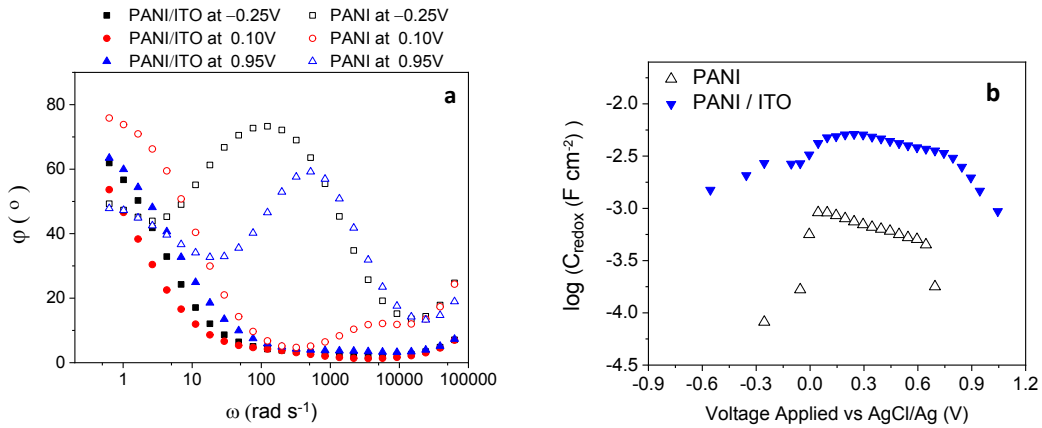

Figure 4. a) Bode phase diagrams at three representative potentials of PANI flat and PANI/ITO-NC electrode. b) Logarithmic dependence of C_{redox} from the applied bias voltage. Electrolyte: 1M $LiClO_4$ in PC.

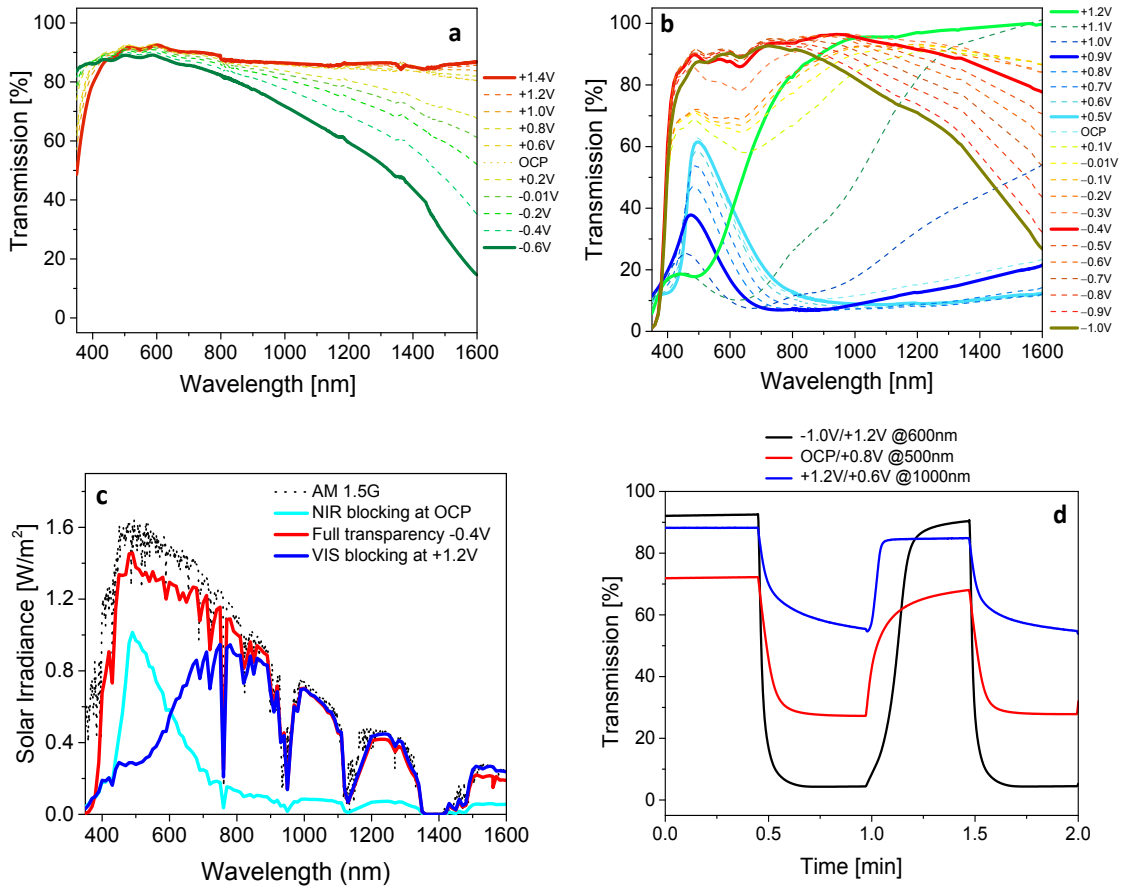

Figure 5. Transmission spectra of (a) bare mesoporous ITO nanocrystalline template and (b) PANI/ITO-NCs electrode polarized at different voltages with respect to AgCl/Ag electrode. (c)

Variation of solar irradiance at different optical states offered by the "plasmochromic" film (d) *In situ* transmittance monitored at various wavelengths by applying square wave perturbation at different voltages (vs. AgCl/Ag).

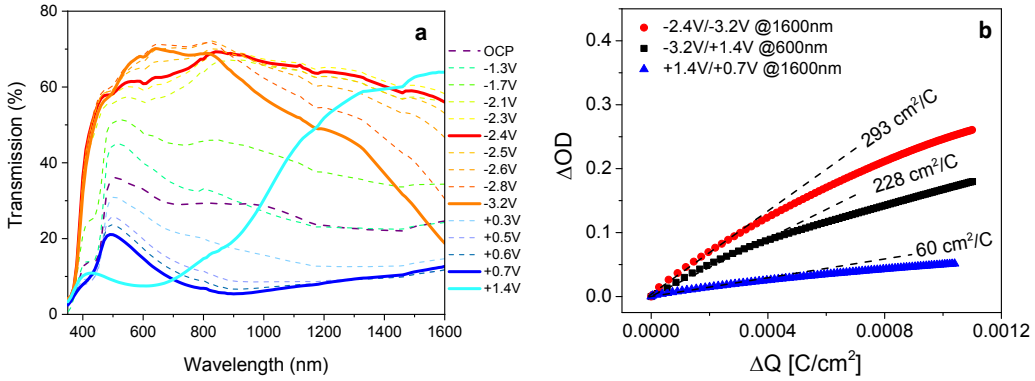

Figure 6. a) Transmittance spectra of the device ITOflat|PANI/ITO-NCs|EL|CeO_2|ITOflat at different applied bias; b) Change in optical density versus the injected charge into the EC device monitored at 600nm and 1600nm.

Table 1. Values of the T_{NIR}, T_{LUM} and T_{SOL} defining the main optical states of the ITO/PANI nanocomposite film

OPTICAL MODE	T_{NIR}	T_{LUM}	T_{SOL}	T_{LUM}/T_{SOL}	ΔV	wavelength (nm)	t_c (s)	t_b (s)
NIR blocking	13%	42%	26%	1.61	OCP / +0.8 V	500	19	6
Full transparency	90%	86%	85%	1.01	-1.0V / +1.2 V	600	4	14
VIS blocking	91%	36%	54%	0.67	+1.2V / +0.6V	1000	7	28